ATMOSPHERIC CIRCULATION ASSOCIATED WITH 3D HEAT WAVE TYPES IN MIDDLE EUROPE

Zuzana Bešťáková[1], Ondřej Lhotka[2,3], Jan Stryhal[2], Jan Kyselý[1,2]

[1] **Faculty of Environmental Sciences**, Czech University of Life Sciences, Prague, Czech Republic; [2] **Institute of Atmospheric Physics**, Czech Academy of Sciences, Prague, Czech Republic; [3] **Global Change Research Institute**, Czech Academy of Sciences, Brno, Czech Republic

This poster will be presented: Thu, 05 Sep, 18:00–19:30

ABSTRACT

We evaluate links between atmospheric circulation and three-dimensional (3D) heat wave types in Middle Europe (one of the PRUDENCE regions) over 1979–2022. Heat waves are classified according to their 3D structure of positive temperature anomalies in ERA5 into near-surface (HWG), lower-tropospheric (HWL), higher-tropospheric (HWH), and omnipresent (HWO) types (Lhotka & Kyselý 2024). The Jenkinson–Collison classification is used to identify circulation types (CTs) with increased frequency during the individual heat wave types, and their climatological characteristics (including mean temperature anomaly, precipitation, and Climatic Water Balance index defined as potential evapotranspiration minus precipitation) are studied in E-OBS data. We show that the mean surface temperature anomalies are largest during HWG (+7.1 °C), while HWL are the driest heat wave type according to mean daily precipitation (0.4 mm). At the same time, HWG types show the driest conditions before their onset. In all heat wave types there is a large increase in the frequency of southern CTs compared to the June–September climatology, but differences among the heat wave types are found for other CTs. In HWG, the most frequent CT is U (undefined), corresponding to little pronounced pressure pattern over Middle Europe with no clear role of anticyclonic circulation or flow direction. The expected pattern of increased anticyclonic and decreased cyclonic flow is clearly manifested only for HWH and to a lesser degree for HWO and HWL types, while it is reversed for HWG. The analysis contributes to a better understanding of the interrelationships between heat waves, atmospheric circulation, and other driving mechanisms.

METHODOLOGY

STUDY AREA & INPUT DATA

- Middle Europe [2–16°E, 48–55°N] (one of the PRUDENCE regions, Christensen & Christensen 2007)
- 1979–2022 period
- extended summer season (June–September)
- 0.1x0.1° long-lat grid boxes
- E-OBS data (temperature, precipitation)
- NCEP/NCAR reanalysis (sea level pressure)
- ERA5 (temperature at 2 m and in 12 vertical levels from 850 up to 300 hPa with 50 hPa step)

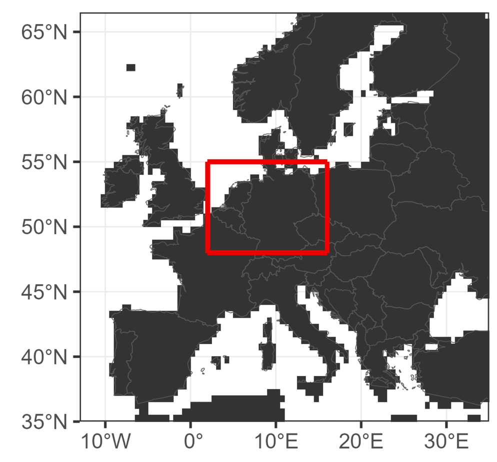

Figure 1: Study area

HEAT WAVES (3D)

- based on 2m temperature data and temperatures at 12 vertical levels
- three vertical layers defined:
  - near-surface (2m temperature)
  - lower troposphere (mean of levels from 850 to 600 hPa)
  - higher troposphere (550 to 300 hPa mean)
- heat wave is defined as a sequence of at least 3 consecutive days when an area of positive temperature anomalies above the 95th percentile was larger than 1/3 of the region in any of the 3 layers (Lhotka & Kyselý 2024)
- based on prevailing locations of temperature anomalies above the 95th percentile, heat waves are classified into 4 types:
  - near-surface (HWG)
  - lower-tropospheric (HWL)
  - higher-tropospheric (HWH)
  - omnipresent (HWO)
- overall 14 HWG, 12 HWL, 14 HWH & 13 HWO identified in the region of Middle Europe over 1979–2022
- mean length 6.2 days for HWG while 3.7–4.2 days for the other heat wave types

CIRCULATION TYPES (CTs)

- Jenkinson & Collison (1977) classification into 26 CTs + U (based on strength, direction and vorticity of flow) for Middle Europe
- CTs were grouped into 11 'supertypes':
  - S = S, CS, AS
  - N = N, CN, AN
  - W= W, CW, AW
  - E = E, CE, AE
  - NE = ANE, CNE, NE
  - SE = ASE, CSE, SE
  - SW = ASW, CSW, SW
  - NW = ANW, CNW, NW
  - A = A
  - C = C
  - U = U

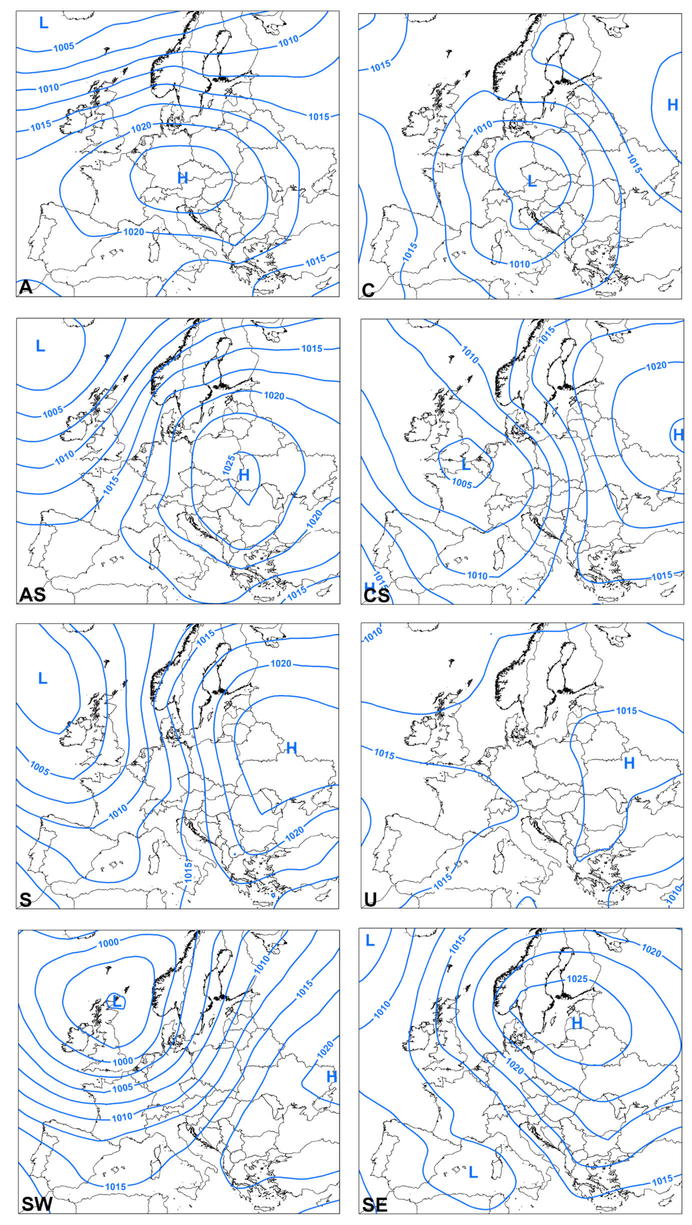

Figure 2: Mean sea-level pressure for 8 out of 27 objectively-derived circulation types centred on Middle Europe (for illustration).

RESULTS

Table 1: Frequency (freq.) of CTs, Cef (efficiency coefficient; ratio of frequency of a given CT in heat waves compared to the mean June–September frequency), dev. TG (temperature anomaly from the mean June–September value of 16.6 °C) and mean precipitation (P) for individual heat wave types. In the bottom row, the mean values of dev. TG and P for days in individual heat wave types are shown.

CT	HWG				HWL				HWH				HWO			
	freq. [%]	Cef [-]	dev. TG [°C]	P [mm/d]	freq. [%]	Cef [-]	dev. TG [°C]	P [mm/d]	freq. [%]	Cef [-]	dev. TG [°C]	P [mm/d]	freq. [%]	Cef [-]	dev. TG [°C]	P [mm/d]
A	**19.57**	**0.88**	6.45	0.17	32.00	1.43	3.89	0.17	**46.15**	**2.07**	1.82	0.28	29.63	1.33	4.10	0.33
AN	–	–	–	–	2.00	0.93	4.91	0.28	–	–	–	–	–	–	–	–
ANE	2.17	2.13	7.48	1.11	–	–	–	–	–	–	–	–	–	–	–	–
AE	–	–	–	–	–	–	–	–	–	–	–	–	–	–	–	–
ASE	2.17	2.89	6.47	0.69	–	–	–	–	–	–	–	–	1.85	2.47	4.91	0.00
AS	2.17	2.47	5.38	0.00	6.00	6.82	5.42	0.00	5.77	6.56	2.97	0.05	1.85	2.10	5.74	0.08
ASW	1.09	0.53	8.07	0.07	–	–	–	–	1.92	0.94	0.64	0.00	9.26	4.52	6.05	0.21
AW	–	–	–	–	–	–	–	–	5.77	1.36	3.28	0.77	3.70	0.87	4.37	1.74
ANW	–	–	–	–	2.00	0.55	2.67	0.66	3.85	1.07	4.40	0.83	–	–	–	–
C	10.87	1.40	7.17	5.30	8.00	1.03	6.13	2.12	3.85	0.50	6.92	2.87	3.70	0.48	7.08	3.97
CN	–	–	–	–	–	–	–	–	–	–	–	–	–	–	–	–
CNE	–	–	–	–	–	–	–	–	1.92	4.47	5.22	0.95	–	–	–	–
CE	1.09	2.32	8.70	1.31	–	–	–	–	–	–	–	–	–	–	–	–
CSE	1.09	1.68	8.16	0.12	–	–	–	–	–	–	–	–	3.70	5.69	8.17	2.74
CS	5.43	7.65	7.54	2.30	2.00	2.82	8.41	0.00	1.92	2.70	6.58	5.75	–	–	–	–
CSW	2.17	1.50	6.97	1.82	–	–	–	–	–	–	–	–	1.85	1.28	6.69	7.14
CW	–	–	–	–	–	–	–	–	–	–	–	–	–	–	–	–
CNW	–	–	–	–	–	–	–	–	–	–	–	–	–	–	–	–
N	–	–	–	–	2.00	0.57	8.76	0.00	1.92	0.55	-1.24	0.13	1.85	0.53	6.29	0.49
NE	–	–	–	–	–	–	–	–	–	–	–	–	–	–	–	–
E	–	–	–	–	6.00	3.70	5.20	0.20	–	–	–	–	–	–	–	–
SE	10.87	4.23	7.08	0.56	6.00	2.33	5.65	0.00	3.85	1.50	5.42	0.81	12.96	5.04	6.10	0.14
S	5.43	1.68	7.27	1.91	12.00	3.70	6.35	0.31	7.69	2.37	5.28	1.45	9.26	2.86	8.17	0.57
SW	–	–	–	–	8.00	1.16	7.92	1.05	5.77	0.84	3.49	3.18	5.56	0.80	7.63	2.51
W	–	–	–	–	2.00	0.21	8.03	0.05	3.85	0.40	4.71	0.70	–	–	–	–
NW	1.09	0.14	8.52	0.23	–	–	–	–	–	–	–	–	1.85	0.24	3.35	10.61
U	34.78	**3.18**	7.42	0.86	12.00	1.10	6.10	0.52	5.77	0.53	5.91	1.95	12.96	1.19	7.62	1.79
mean	–	–	7.13	1.29	–	–	5.49	0.44	–	–	3.19	0.91	–	–	5.96	1.21

Table 2: Same as Table 1, but for 11 'supertypes' (A; C; N = N, CN, AN; NE = NE, CNE, ANE; E = E, CE, AE; SE = SE, CSE, ASE; S = S, CS, AS; SW = SW, CSW, ASW; W = W, CW, AW; NW = NW, CNW, ANW; U). In the far right box the mean seasonal frequency (freq.), temperature anomaly (dev. TG), and daily precipitation (P) for June–September 1979–2022 are shown.

CT	HWG				HWL				HWH				HWO				June–September		
	freq. [%]	Cef [-]	dev. TG [°C]	P [mm/d]	freq. [%]	Cef [-]	dev. TG [°C]	P [mm/d]	freq. [%]	Cef [-]	dev. TG [°C]	P [mm/d]	freq. [%]	Cef [-]	dev. TG [°C]	P [mm/d]	freq. [%]	dev. TG [°C]	P [mm/d]
A	**19.57**	**0.88**	6.45	0.17	32.00	1.43	3.89	0.17	**46.15**	**2.07**	1.82	0.28	29.63	1.33	4.10	0.33	22.30	-0.29	0.47
C	10.87	1.40	7.17	5.30	8.00	1.03	6.13	2.12	3.85	0.50	6.92	2.87	3.70	0.48	7.08	3.97	7.70	0.03	5.49
N	–	–	–	–	4.00	0.66	6.84	0.14	1.92	0.31	-1.24	0.13	1.85	0.30	6.29	0.49	6.10	-1.90	2.88
NE	2.17	0.70	7.48	1.11	–	–	–	–	1.92	0.62	5.22	0.95	–	–	–	–	3.10	-0.99	2.08
E	1.09	0.36	8.70	1.31	6.00	2.00	5.20	0.20	–	–	–	–	–	–	–	–	3.00	0.47	1.00
SE	14.13	3.53	7.07	0.55	6.00	1.50	5.65	0.00	3.85	0.96	5.42	0.81	18.52	4.63	6.39	0.65	4.00	2.18	1.08
S	13.04	2.72	7.07	1.76	20.00	4.17	6.28	0.19	15.38	3.20	4.58	1.46	11.11	2.31	7.77	0.49	4.80	2.35	1.72
SW	3.26	0.31	7.33	1.23	8.00	0.77	7.92	1.05	7.69	0.74	2.77	2.39	16.67	1.60	6.65	1.75	10.40	1.01	2.98
W	–	–	–	–	2.00	0.13	8.03	0.05	9.62	0.62	3.85	0.74	3.70	0.24	4.37	1.74	15.40	-0.56	2.90
NW	1.09	0.09	8.52	0.23	2.00	0.16	2.67	0.66	3.85	0.32	4.40	0.83	1.85	0.15	3.35	10.61	12.20	-1.93	2.62
U	34.78	**3.18**	7.42	0.86	12.00	1.10	6.10	0.52	5.77	0.53	5.91	1.95	12.96	1.19	7.62	1.79	10.90	1.93	2.40

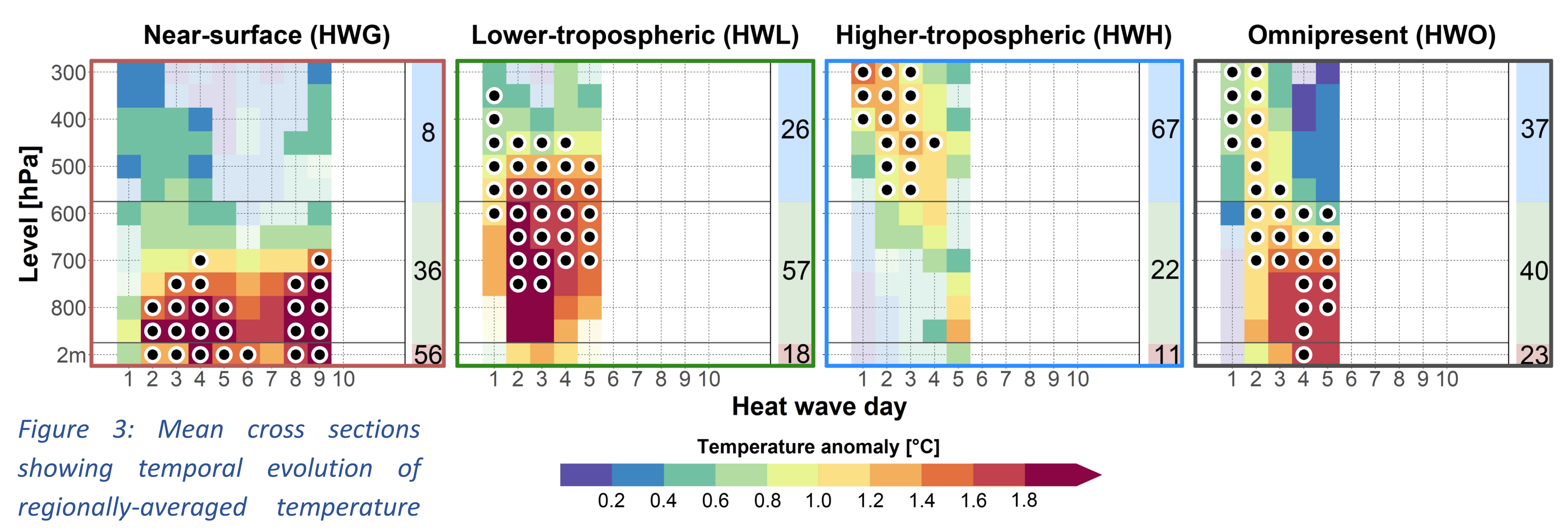

Figure 3: Mean cross sections showing temporal evolution of regionally-averaged temperature anomalies (TA) above the 95th percentile of summertime daily temperature distribution. Dots = positive TA occurred in >50% of the region; pale shading = TA over <25% of the domain. Numbers stand for mean proportions [%] of positive TA (intensity and spatial extent combined) in near-surface (red), lower-tropospheric (green), and higher-tropospheric (blue) layers.

Source: Lhotka & Kyselý (2024)

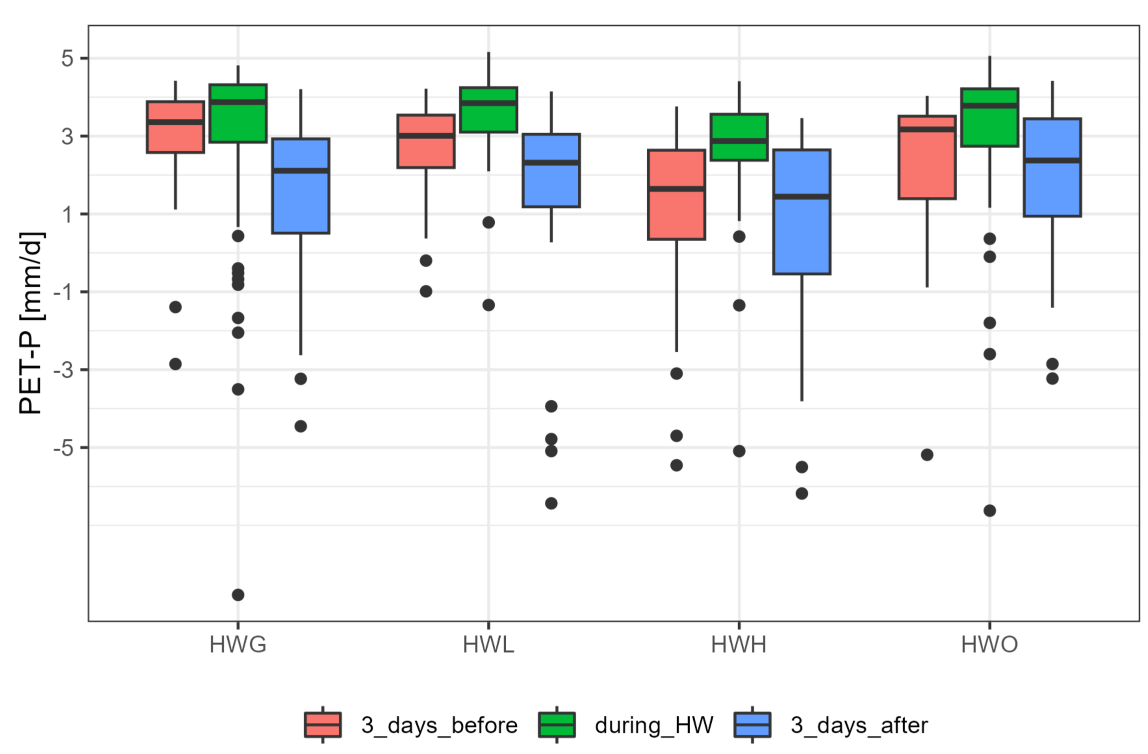

Figure 4: Differences between PET and precipitation (P) for individual heat wave types on three days before, during, and three days after heat waves. The black line in the boxplots shows the median.

SUMMARY

- the individual heat wave types differ in many characteristics including their vertical cross sections (Figure 3)
- HWG types are the longest and show the driest conditions before heat wave onset (Figure 4)
- the surface temperature anomalies are largest during HWG (**+7.1 °C**) while they are much smaller for HWH (+3.2 °C) (Table 1)
- HWL are the driest heat wave type, with mean daily precipitation only **0.4 mm**, while HWG and HWO are the wettest (1.2-1.3 mm)
- in all heat wave types there is a large increase in frequency of southern CTs compared to the June–September climatology but differences between heat wave types are found for other CTs (Tables 1 & 2):
  - in HWG, the most frequent CT is U (undefined), corresponding to little pronounced pressure pattern over Middle Europe, with no clear role of anticyclonic circulation (A is less frequent compared to climatology while C more frequent)
  - the role of anticyclonic circulation increases for HWL, HWO and particularly HWH (A type occurs on nearly half of the days in HWH, compared to less than 20% in HWG)
  - warm southerly advection is important in all heat wave types, mainly HWL and HWH; southeasterly advection mainly in HWO and HWG
  - northerly and westerly flow is reduced in all heat wave types, and except for HWL, this concerns also easterly flow
- flow direction and warm advection is more important than vorticity for HWG, and to some extent also for HWL
- the (expected) pattern of increased anticyclonic and decreased cyclonic flow is clearly manifested only for HWH and to lesser degree for HWO and HWL types while it is reversed for HWG

REFERENCES:

Christensen J. H. & Christensen O. B. (2007) A summary of the PRUDENCE model projections of changes in European climate by the end of this century. Climatic Change 81, 7–30

Jenkinson A.F. & Collison B. P. (1977) An initial climatology of gales over the North Sea. Synoptic Climatology Branch Memorandum 62, Meteorological Office, London, UK. 18 pp

Lhotka O. & Kyselý J. (2024) Three-dimensional structures of European heat waves (2024). Comm. Earth & Environment 5, 1–8. (link)

contact: bestakova@fzp.czu.cz, ondrej.lhotka@ufa.cas.cz